Reliable Low-Rank Approximation of Matrices Detection Aided Multicarrier DCSK Receiver Design

Lin Zhang, *Senior Member, IEEE*, Jieheng Zheng, Bingjun Chen, and Zhiqiang Wu, *Senior Member, IEEE*

***Abstract*—Multicarrier differential chaos shift keying (MC-DCSK) systems transmit the reference chaotic signal for information recovery to remove the complex synchronization circuit. However, transmission errors in the reference chaotic signal would induce the error propagations when directly used for demodulations. In order to address this issue, we propose a low-rank approximation of matrices (LRAM) detection method to improve the reliability performances. In our design, we exploit the low-rank characteristic of MC-DCSK signals sharing the reference chaotic signal. Instead of directly using the received reference chaotic signal for correlated demodulation, we propose to apply the LRAM method to jointly estimate the reference signal and the information-bearing signal. We use the singular value decomposition and generalized LRAM methods to minimize the distances between the estimates and transmitted data. Thus, the signal-to-noise ratio (SNR) can be improved to achieve lower bit error rate (BER). Moreover, theoretical BER expression is derived and LRAM-aided system is proved to be capable of proving the maximum-likelihood detection for received signals. Simulation results demonstrate the BER performances of our design outperform counterparts over additive white Gaussian noise and fading channels.**

***Index Terms*—Low-rank approximation of matrices (LRAM), maximum-likelihood detection, multicarrier differential chaos shift keying (MC-DCSK), reliability, singular value decomposition (SVD).**

I. Introduction

In THE past few decades, chaotic transmissions have been widely applied in wireless systems to enhance the security performances and the antijamming capability [1] thanks to the properties of chaotic sequences including being sensitive to the initial value, nonpredictable and nonperiodic [2], [3]. Moreover, the deterministic features of transmitted signals can be effectively hidden behind apparent irregular chaotic behavior.

According to whether the reference chaotic signal is transmitted, chaotic modulations are classified into coherent modulations and noncoherent modulations [4], [5]. Since noncoherent modulation schemes remove the complex chaotic synchronization circuit required by the coherent chaotic modulation, they have attracted more research interests.

Among noncoherent chaotic modulations, the differential chaos shift keying (DCSK) [6] scheme demonstrates better performances than another noncoherent chaotic modulation scheme, which is correlation delay shift keying [7], and has been widely investigated. However, as mentioned in [8], DCSK systems have two main drawbacks. One is low energy and spectrum efficiencies since only half the bit duration is spent on the information transmission. Another is the need for radio frequency delay circuit at the receiver, which is not easy to implement in practical systems.

To address these issues, multicarrier (MC) transmission has been applied in DCSK systems, and improved DCSK schemes have been recently proposed in [8]–[11]. In these schemes, the reference chaotic signal is transmitted over a predefined subcarrier frequency, and multiple data-bearing signals shared the same reference are transmitted over the remaining subcarriers. Thus the impractical delay circuit applied in the traditional DCSK system is removed. Moreover, since multiple data-bearing chaotic modulated signals share the same reference chaotic signal, both spectrum and energy efficiencies are improved.

Thanks to these advantages, in recent years, many variants of MC-DCSK have been proposed to improve the performances further. For example, the carrier index DCSK (CI-DCSK) [12], the permutation index DCSK (PI-DCSK) [13], and the commutation code index DCSK (CCI-DCSK) [14]–[16] systems are proposed to perk up efficiencies by utilizing the chip index of chaotic sequences. Explicitly, in [12], the CI-DCSK systems transmit more information in each bit duration by constructing the one-to-one mapping between carrier activation patterns and index symbols. Different from CI-DCSK, the PI-DCSK systems [13] select one of the predefined reference sequence permutations to spread modulated symbols. In [14], orthogonal signals are constructed by reverting the reference chaotic signals and by transforming the reference to the orthogonal version with the aid of the CCI. Besides, in [17], a low-complexity superposition coding PPM-DCSK scheme is proposed for downlink multiuser chaotic communications. In our recent research work, we propose an overlapped chaotic chip position shift keying system to enhance the security and the efficiency of MC-DCSK systems [18]. Besides, we propose to utilize the frequency and time diversity to enhance the security and the robustness performances while not requiring channel state information to be known at the receiver [19].

In order to enhance the reliability performances of MC-DCSK systems, a few research works have been conducted. For instance, the subcarrier allocated MC-DCSK (SA-MCDCSK)

Manuscript received May 7, 2020; revised September 21, 2020; accepted December 6, 2020. Date of publication December 30, 2020; date of current version December 9, 2021. This work was supported by the National Key Research and Development Program of China under Grant 2018YFB1802300. *(Corresponding author: Lin Zhang.)*

Lin Zhang is with the School of Electronics and Information Technology, Sun Yat-sen University, Guangzhou 510006, China and also with the Southern Marine Science and Engineering Guangdong Laboratory, Zhuhai 519000, China (e-mail: isszl@mail.sysu.edu.cn).

Jieheng Zheng and Bingjun Chen are with the School of Electronics and Information Technology, Sun Yat-sen University, Guangzhou 510006, China (e-mail: z_jack_heng@126.com; cbigdream@qq.com).

Zhiqiang Wu is with the Tibet University, Lhasa 850000, China and also with the Department of Electrical Engineering, Wright State University, DaytonOH 45435 USA (e-mail: zhiqiang.wu@wright.edu).

Digital Object Identifier 10.1109/JSYST.2020.3043420

system [20] can achieve better bit error rate (BER) performances by allocating more subcarriers to reference signals; thus the noise of reference signal can be reduced by utilizing diversity at the cost of bandwidth efficiency. In our previous work [21], we also proposed a noise-suppressing chaos generator to enhance the reliability performances for chaotic communication systems.

However, these methods for reliability enhancement require to modify the transmitter structure. In our recent research work [22], we proposed a generalized iterative receiver with no requirement for transmitter structure modifications. With this design, the reliability of information transmission is improved by performing correlated demodulation with more reliable reference chaotic signal, since higher signal-to-noise ratio (SNR) ratio could be achieved to enhance the BER performances.

Different from the existing improved chaotic modulation schemes that require to modify the transmitter, or our iterative receiver design requiring the feedback branch at the receiver, in this article, neither modifications of transmitters nor the feedback branch is required. In our design, unlike the traditional receivers that directly recover the information with the reference chaotic signal received, we propose to apply the low-rank approximation of matrices (LRAM) method to jointly retrieve the reference signal and the information-bearing signal from received signals. Explicitly, we propose to utilize the special low-rank characteristic of transmitted MC-DCSK signal matrices to detect the information-bearing chaotic modulated signals jointly at the receiver. Only an additional detection module is added to the MC-DCSK receiver to achieve the maximum-likelihood detection of received signals.

In our design, we propose to attain the estimates using the LRAM detection methods. Since one reference chaotic symbol can be shared by part of or all the other information-bearing chaotic modulated symbols at the MC-DCSK transmitter, the transmitted signal matrix sharing the same one reference chaotic signal will have a rank of one. Accordingly, at the MC-DCSK receiver, the detected information-bearing chaotic modulated signals are expected to have the rank as low as possible.

We first represent the received signals as the sum of the information-bearing chaotic modulated signal matrix and a noise matrix. Then, we utilize the LRAM detection methods [23]–[26], including the singular value decomposition (SVD) and the generalized low-rank approximations of matrices (GLRAM) methods, to evaluate the information-bearing chaotic modulated signals. Moreover, we provide the theoretical proof that the LRAM detection aided system can achieve the maximum-likelihood detection of reference chaotic signals, thereby attaining the best BER performances for MC-DCSK systems. Simulation results demonstrate that the proposed LRAM detection aided MC-DCSK receiver design achieves better reliability performances over additive white Gaussian noise (AWGN) channel and fading channels than benchmark schemes.

Briefly, the main contributions include the following.

1) We propose to utilize the low-rank characteristic of the noncoherent MC-DCSK transmitted signals and propose an LRAM detection aided MC-DCSK receiver to improve the SNR of the reference chaotic signals and the information-bearing chaotic modulated signals. As a result, reliability performances will be enhanced.
2) Two LRAM methods, i.e., the SVD and the GLRAM methods, are utilized to recover the chaotic modulated symbols at the receiver while not requiring to modify the transceiver structure. Besides, we prove that the LRAM reception scheme can achieve the maximum-likelihood detection of the reference chaotic signal.
3) We analyze the theoretical BER performances and compare the complexity among the proposed system and counterpart systems. Then simulation results are provided over AWGN and fading channels to validate our design, which demonstrates that our proposed receiver attains better reliability performances than benchmark systems.

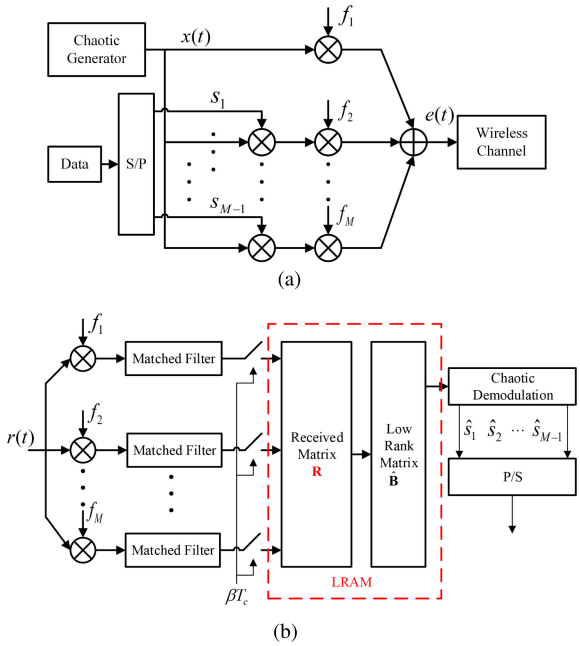

Fig. 1. Block diagram of the LRAM detection aided MC-DCSK transceiver. (a) LRAM detection aided MC-DCSK transmitter. (b) LRAM detection aided MC-DCSK receiver.

The rest of this article is organized as follows. Section II presents the LRAM detection aided MC-DCSK transceiver, and then Section III provides details of the proposed receiver and two LRAM methods used for data recovery. Subsequently, we provide the theoretical BER performance analysis and the complexity analysis in Section IV, and the simulations are performed in Section V to investigate BER performances over AWGN channel and fading channels. Finally, Section VI concludes the article.

II. System Model of MC-DCSK With Receiver Based on LRAM

In this section, we will present the LRAM detection aided MC-DCSK transceiver structure.

A. MC-DCSK Transmitter

In our design, the MC-DCSK transmitter structure remains the same as that in [10] to be compatible with existing systems.

As shown in Fig. 1(a), on the one hand, the chaos generator uses a second-order Chebyshev map [27] to generate a chaotic sequence $[x_1, x_2, \ldots, x_\beta]$ represented by

$$x_{\mu+1} = 1 - 2x_\mu^2 \tag{1}$$

where β represents the length of the chaotic sequence, x_μ is the μth element of the chaotic sequence, $x_\mu \in (-1, 1), \mu = 1, 2, \ldots, \beta$, and x_1 is the initial value predefined. Then, square-root-raised-cosine filters are applied to combat the intersymbol interference (ISI), which generates the chaotic spreading signal $x(t)$ expressed as

$$x(t) = \sum_{k=1}^{\beta} x_k g(t - kT_c) \tag{2}$$

where T_c is the chip time and βT_c is the duration of a bit, and $g(t)$ is the square-root-raised-cosine filter.

On the other hand, the binary information bits are modulated by the binary phase-shift keying (BPSK). Then, the serial BPSK symbols are converted into parallel data sequence $[s_1, s_2, \ldots, s_{M-1}]$, where M is the number of subcarriers.

Subsequently, $[s_1, s_2, \ldots, s_{M-1}]$ is modulated by $x(t)$. Then, $x(t)$ is transmitted via a single specific subcarrier, whereas the chaotic modulated signals are transmitted over the remaining $M-1$ subcarriers. Namely, the reference chaotic signal and the information-bearing chaotic modulated signals are combined to constitute the signal $e(t)$ to be delivered over channels, which is represented by [10]

$$e(t) = x(t)\cos(2\pi f_1 t + \phi_1) + \sum_{i=2}^{M} s_{i-1} x(t)\cos(2\pi f_i t + \phi_i) \tag{3}$$

where f_i and ϕ_i represent the frequency and phase angle introduced during the ith subcarrier modulation process. Note that the items $s_{i-1}x(t)$ in (3) delivered via different subcarriers are linearly correlated with each other, due to the modulation with the same reference chaotic signal $x(t)$. Hence, the transmitted signal matrix will have a rank of 1.

B. LRAM Detection-Based MC-DCSK Receiver

Fig. 1(b) shows the LRAM detection-based MC-DCSK receiver structure. At the receiver, the received signal can be represented as

$$r(t) = \int_{-\infty}^{\infty} h(\tau, t) e(t - \tau) d\tau + n(t) \tag{4}$$

where $r(t)$ is the received signal and $n(t)$ is the AWGN noise with a variance of $N_0/2$ and zero mean. Additionally, $h(\tau, t)$ represents the channel response.

For a fast frequency-selective fading channel, $h(\tau, t)$ can be expressed as a linear time-varying model [28] given by

$$h(\tau, t) = \sum_{l=1}^{L} h_l(t)\delta(\tau - \tau_l(t)) \tag{5}$$

where $h_l(t)$ and $\tau_l(t)$ are the channel coefficient and the delay of the lth path. Meanwhile, L is the total number of paths. In addition, for the slow fading channel, the channel response is expressed as $h(\tau) = \sum_{l=1}^{L} h_l \delta(\tau - \tau_l)$, whereas for the flat fading channels, $L = 1$, thus we have $h(\tau, t) = h_0(t)\delta(\tau - \tau_0(t))$.

Then after the square-root-raised cosine filtering and sampling every βT_c time slots, the resultant received symbols are represented as a symbol matrix $\mathbf{R} = [\mathbf{R_1}, \mathbf{R_2}, \ldots, \mathbf{R_M}]$, wherein $\mathbf{R_1}$ represents the received chaotic signal, whereas $\mathbf{R_2}, \ldots, \mathbf{R_M}$ are received information-bearing chaotic modulated signals. Moreover, the jth received symbol in $\mathbf{R_m}$ over the multipath fast fading channel, which is denoted by $r_{j,m}$, can be expressed as

$$r_{j,m} = \left(\sum_{l=1}^{L} h_j^{(l)} x_{j-\tau_j^{(l)}} \right) s_m + n_{j,m} \tag{6}$$

where $j = 1, 2, \ldots, \beta$, $m = 0, 1, \ldots, M-1$, $h_j^{(l)}$ and $\tau_j^{(l)}$, respectively, denote the channel coefficient and the time delay of the lth path, s_m is the mth transmitted symbol, and $s_0 = 1$ when delivering the reference chaotic symbol.

Then, we write $\mathbf{R}$ as the summation of two matrices, which, respectively, represent the information bearing submatrix $\mathbf{B}$ and the noise submatrix $\mathbf{N}$, i.e.,

$$\mathbf{R} = \mathbf{B} + \mathbf{N} \tag{7}$$

where $\mathbf{B}$ is represented as (8), shown at the bottom of this page, whereas $\mathbf{N}$ is denoted by

$$\mathbf{N} = \begin{pmatrix} n_{1,0} & n_{1,1} & \cdots & n_{1,M-1} \\ \vdots & \vdots & \ddots & \vdots \\ n_{\beta,0} & n_{\beta,1} & \cdots & n_{\beta,M-1} \end{pmatrix}. \tag{9}$$

It can be seen from (8) that the first column vector is correlated with the other column vectors; therefore, $\mathbf{B}$ has the rank of 1. Then, we propose extract the estimate $\hat{\mathbf{B}}$ of $\mathbf{B}$ from the received symbol matrix $\mathbf{R}$. Since the rank of $\mathbf{B}$ is 1, naturally $\hat{\mathbf{B}}$ is expected to have a rank as low as 1. Let $\hat{\mathbf{b}}_i$ represent the ith column vector, $i = 1, 2, \ldots, M$, then the matrix $\hat{\mathbf{B}}$ can be obtained via the LRAM detection as

$$\hat{\mathbf{B}} = [\hat{\mathbf{b}}_1, \hat{\mathbf{b}}_2, \ldots, \hat{\mathbf{b}}_M]. \tag{10}$$

$$\begin{aligned} \mathbf{B} &= \begin{pmatrix} \sum_{l=1}^{L} h_1^{(l)} x_{1-\tau_1^{(l)}} & \left(\sum_{l=1}^{L} h_1^{(l)} x_{1-\tau_1^{(l)}} \right) s_1 \cdots \left(\sum_{l=1}^{L} h_1^{(l)} x_{1-\tau_1^{(l)}} \right) s_{M-1} \\ \vdots & \vdots \quad \ddots \quad \vdots \\ \sum_{l=1}^{L} h_\beta^{(l)} x_{\beta-\tau_\beta^{(l)}} & \left(\sum_{l=1}^{L} h_\beta^{(l)} x_{\beta-\tau_\beta^{(l)}} \right) s_1 \cdots \left(\sum_{l=1}^{L} h_\beta^{(l)} x_{\beta-\tau_\beta^{(l)}} \right) s_{M-1} \end{pmatrix} \\ &= \left(\sum_{l=1}^{L} h_1^{(l)} x_{1-\tau_\beta^{(l)}} \cdots \sum_{l=1}^{L} h_\beta^{(l)} x_{\beta-\tau_\beta^{(l)}} \right)^T (s_0 s_1 \cdot s_{M-1}) \end{aligned} \tag{8}$$

Finally, the correlated chaotic demodulation is conducted with $\hat{\mathbf{b}}_1$ obtained from the LRAM detection. Namely, for the ith symbol, the demodulated symbol could be derived by $\hat{\mathbf{b}}_1 \cdot \hat{\mathbf{b}}_{i+1}$. Then, the symbol estimate can be obtained as

$$\hat{s}_i = \mathrm{sgn}(\hat{\mathbf{b}}_1 \cdot \hat{\mathbf{b}}_{i+1}) \tag{11}$$

where $i = 1, \ldots, M-1$, $\mathrm{sgn}(\cdot)$ is the function that returns an integer indicating the sign of a number, and $(\cdot)$ means the inner product operation.

III. LRAM-Aided Information Detection Design

In this section, we will present the LRAM-based detection scheme, and prove the maximum-likelihood detection could be achieved. Besides, two SVD and GLRAM methods are presented.

A. LRAM-Aided Information Detection Design for MC-DCSK Receivers

1) LRAM-Aided Detection Design: As presented in [29], the optimal rank-k approximation of matrix $\mathbf{R}$, i.e., $\hat{\mathbf{B}}$, can be calculated by

$$\hat{\mathbf{B}} = \underset{\mathrm{rank}(\hat{\mathbf{B}})=k}{\arg\min} \left\|\mathbf{R}-\hat{\mathbf{B}}\right\|_F = \underset{\mathrm{rank}(\hat{\mathbf{B}})=k}{\arg\min} \left\|\mathbf{B}+\mathbf{N}-\hat{\mathbf{B}}\right\|_F \tag{12}$$

where the Frobenius norm F of a matrix $\mathbf{Z}$ is given by $\|\mathbf{Z}\|_F = \sqrt{\sum_{i,j} Z_{i,j}^2}$. As mentioned above, the rank of $\mathbf{B}$ is 1, the rank of $\hat{\mathbf{B}}$ is expected to be as low as 1, namely $\mathrm{rank}(\hat{\mathbf{B}}) = k = 1$.

To be more explicit, let $\mathbf{b_j}$ and $\hat{\mathbf{b}}_\mathbf{j}$, respectively, denote the jth column vector of $\mathbf{B}$ and its approximation matrix $\hat{\mathbf{B}}$. Then, $\hat{\mathbf{b}}_\mathbf{1}$ denotes the first column vector in $\hat{\mathbf{B}}$, and $\hat{\mathbf{b}}_\mathbf{1}$ is the approximate value of the vector $\mathbf{b_1}$ in $\mathbf{B}$ given in (8), which corresponds to the received reference chaotic sequence.

2) Proof of the Maximum-Likelihood Detection: Next, we will prove that by solving $\arg\min_{\mathrm{rank}(\hat{\mathbf{B}})=1} \|\mathbf{R}-\hat{\mathbf{B}}\|_F$, the maximum-likelihood detection of the reference chaotic signal can be achieved, i.e., we can obtain $\arg\min_{\hat{\mathbf{b}}_1} \|\mathbf{b}_1 - \hat{\mathbf{b}}_1\|^2$. Namely, we will prove that

$$\underset{\mathrm{rank}(\hat{\mathbf{B}})=1}{\arg\min} \left\|\mathbf{R}-\hat{\mathbf{B}}\right\|_F \Leftrightarrow \underset{\hat{\mathbf{b}}_1}{\arg\min} \left\|\mathbf{b}_1-\hat{\mathbf{b}}_1\right\|^2. \tag{13}$$

First, we prove Theorem 1.

Theorem 1:

$$\underset{\mathrm{rank}(\hat{\mathbf{B}})=1}{\arg\min} \left\|\mathbf{R}-\hat{\mathbf{B}}\right\|_F \Leftrightarrow \underset{\hat{\mathbf{b}}_j}{\arg\max} \left(\sum_{j=1}^{M} \left(\mathbf{b}_j \cdot \hat{\mathbf{b}}_j\right)\right). \tag{14}$$

Proof: Under the condition of $\mathrm{rank}(\hat{\mathbf{B}}) = k = 1$, by applying the square operation, (12) can be expressed as

$$\begin{aligned} &\underset{\mathrm{rank}(\hat{\mathbf{B}})=1}{\arg\min} \left\|\mathbf{R}-\hat{\mathbf{B}}\right\|_F \Leftrightarrow \underset{\mathrm{rank}(\hat{\mathbf{B}})=1}{\arg\min} \left\|\mathbf{R}-\hat{\mathbf{B}}\right\|_F^2 \\ &\Leftrightarrow \underset{\mathrm{rank}(\hat{\mathbf{B}})=1}{\arg\min} \left\|\mathbf{B}+\mathbf{N}-\hat{\mathbf{B}}\right\|_F^2. \end{aligned} \tag{15}$$

Let $B_{i,j}$, $\hat{B}_{i,j}$, and $N_{i,j}$, respectively, represent the element in the ith row and the jth column of $\mathbf{B}$, $\hat{\mathbf{B}}$, and $\mathbf{N}$. By combining the expression of Frobenius norm, the optimization objective in (15) can be expressed as

$$\begin{aligned} &\underset{\mathrm{rank}(\hat{\mathbf{B}})=1}{\arg\min} \left\|\mathbf{B}+\mathbf{N}-\hat{\mathbf{B}}\right\|_F^2 \\ &\Leftrightarrow \underset{B_{i,j}}{\arg\min} \left(\sum_{i=1}^{\beta}\sum_{j=1}^{M} \left(B_{i,j}+N_{i,j}-\hat{B}_{i,j}\right)^2\right) \\ &\Leftrightarrow \underset{B_{i,j}}{\arg\min} \left(\sum_{i=1}^{\beta}\sum_{j=1}^{M} \left[\left(B_{i,j}-\hat{B}_{i,j}\right)^2 + N_{i,j}^2 \right.\right. \\ &\qquad \left.\left. + 2B_{i,j}N_{i,j} - 2\hat{B}_{i,j}N_{i,j}\right]\right). \end{aligned} \tag{16}$$

Since chaotic signals are weakly correlated with noise signals, the correlation value between the chaotic sequence and the noise sequence is close to zero, especially when β is large. Therefore, we can obtain that

$$\mathbf{b}_j \cdot \mathbf{n}_j = \sum_{i=1}^{\beta} B_{i,j}N_{i,j} \approx 0; \quad \hat{\mathbf{b}}_j \cdot \mathbf{n}_j = \sum_{i=1}^{\beta} \hat{B}_{i,j}N_{i,j} \approx 0 \tag{17}$$

where $\mathbf{b_j}$, $\hat{\mathbf{b}}_\mathbf{j}$, and $\mathbf{n_j}$, respectively, denote the jth column vector of $\mathbf{B}$, its approximation matrix $\hat{\mathbf{B}}$, and noise matrix $\hat{\mathbf{N}}$. Then, we can obtain

$$\begin{aligned} &\underset{B_{i,j}}{\arg\min} \left(\sum_{i=1}^{\beta}\sum_{j=1}^{M} \left[\left(B_{i,j}-\hat{B}_{i,j}\right)^2 + N_{i,j}^2 \right.\right. \\ &\qquad \left.\left. + 2B_{i,j}N_{i,j} - 2\hat{B}_{i,j}N_{i,j}\right]\right) \\ &\Leftrightarrow \underset{B_{i,j}}{\arg\min} \left(\sum_{i=1}^{\beta}\sum_{j=1}^{M} \left[\left(B_{i,j}-\hat{B}_{i,j}\right)^2 + N_{i,j}^2\right]\right). \end{aligned} \tag{18}$$

Thus, substituting (18) into (16), we obtain

$$\begin{aligned} &\underset{\mathrm{rank}(\hat{\mathbf{B}})}{\arg\min} \left\|\mathbf{B}+\mathbf{N}-\hat{\mathbf{B}}\right\|_F^2 \\ &\Leftrightarrow \underset{B_{i,j}}{\arg\min} \left(\sum_{i=1}^{\beta}\sum_{j=1}^{M} \left[B_{i,j}^2 + \hat{B}_{i,j}^2 + N_{i,j}^2 - 2B_{i,j}\hat{B}_{i,j}\right]\right). \end{aligned} \tag{19}$$

Considering that the normalization is applied to maintain the power as a constant, we can get

$$\sum_{i=1}^{\beta} B_{i,j}^2 = \sum_{i=1}^{\beta} \hat{B}_{i,j}^2 = 1; \qquad \sum_{i=1}^{\beta} N_{i,j}^2 = \sigma^2 \tag{20}$$

where σ^2 is the noise variance. Substituting (20) into (19), the optimization issue can be approximated by

$$\underset{\mathrm{rank}(\hat{\mathbf{B}})}{\arg\min} \left\|\mathbf{B}+\mathbf{N}-\hat{\mathbf{B}}\right\|_F^2$$

$$\Leftrightarrow \arg\min_{B_{i,j}} \left(2M + \sigma^2 M - \sum_{i=1}^{\beta} \sum_{j=1}^{M} 2B_{i,j}\hat{B}_{i,j} \right)$$

$$\Leftrightarrow \arg\min_{\hat{\mathbf{b}}_j} \left(2M + \sigma^2 M - \sum_{j=1}^{M} 2\left(\mathbf{b}_j \cdot \hat{\mathbf{b}}_j\right) \right)$$

$$\Leftrightarrow \arg\max_{\hat{\mathbf{b}}_j} \left(\sum_{j=1}^{M} \left(\mathbf{b}_j \cdot \hat{\mathbf{b}}_j\right) \right). \quad (21)$$

Then, from (15) and (21), we can derive that

$$\arg\min_{\mathrm{rank}(\hat{\mathbf{B}})=1} \left\| \mathbf{R} - \hat{\mathbf{B}} \right\|_F \Leftrightarrow \arg\max_{\hat{\mathbf{b}}_j} \left(\sum_{j=1}^{M} \left(\mathbf{b}_j \cdot \hat{\mathbf{b}}_j\right) \right). \quad (22)$$

□

3) Implementation of the Maximum-Likelihood Detection: According to Theorem 1, the problem of finding the optimal $\hat{\mathbf{B}}$ for $\arg\min_{\mathrm{rank}(\hat{\mathbf{B}})=1} \|\mathbf{R} - \hat{\mathbf{B}}\|_F$ is converted to solving the problem $\arg\max_{\hat{\mathbf{b}}_j}(\sum_{j=1}^{M}(\mathbf{b}_j \cdot \hat{\mathbf{b}}_j))$, which means that the LRAM detection module aims to maximize the correlation value between corresponding column vector pairs, i.e., $\mathbf{b}_j$ and $\hat{\mathbf{b}}_j$ of $\mathbf{B}$ and $\hat{\mathbf{B}}$.

Next, since the first column vector, i.e., $\hat{\mathbf{b}}_1$ represents the estimates of the reference chaotic signal $\mathbf{b}_1$, whereas the other column vectors $\hat{\mathbf{B}}$ are all correlated with $\hat{\mathbf{b}}_1$, the correlation maximization problem can be equivalently converted to the minimization of the difference between the column vector pair, i.e., $\mathbf{b}_1$ and $\hat{\mathbf{b}}_1$. We will prove that $\arg\max_{\hat{\mathbf{b}}_j}(\sum_{j=1}^{M}(\mathbf{b}_j \cdot \hat{\mathbf{b}}_j)) \Leftrightarrow \arg\min_{\hat{\mathbf{b}}_1} \|\mathbf{b}_1 - \hat{\mathbf{b}}_1\|^2$ in detail in Theorem 2.

Theorem 2:

$$\arg\max_{\hat{\mathbf{b}}_j} \left(\sum_{j=1}^{M} \left(\mathbf{b}_j \cdot \hat{\mathbf{b}}_j\right) \right) \Leftrightarrow \arg\min_{\hat{\mathbf{b}}_1} \left\| \mathbf{b}_1 - \hat{\mathbf{b}}_1 \right\|^2. \quad (23)$$

Proof: Similar to $\mathbf{B}$, we normalize $\hat{\mathbf{B}}$ as $||\hat{\mathbf{b}}_1|| = ||\mathbf{b}_1|| = 1$.

According to (7), the jth column vector of $\mathbf{R}$ is $\mathbf{b}_j + \mathbf{n}_j$. In the LRAM detection module, $\hat{\mathbf{B}}$ can be regarded as the projection of $\mathbf{R}$ in a one-dimensional (1-D) space. Thus, the jth column vector of $\hat{\mathbf{B}}$ is expressed as the projection of $\mathbf{R}$ via

$$\hat{\mathbf{b}}_j = \frac{(\mathbf{b}_j + \mathbf{n}_j) \cdot \hat{\mathbf{b}}_1}{(\mathbf{b}_1 + \mathbf{n}_1) \cdot \hat{\mathbf{b}}_1} \hat{\mathbf{b}}_1. \quad (24)$$

Then, we have

$$\arg\max_{\hat{\mathbf{b}}_j} \left(\sum_{j=1}^{M} \left(\mathbf{b}_j \cdot \hat{\mathbf{b}}_j\right) \right) = \arg\max_{\hat{\mathbf{b}}_j} \left(\sum_{j=1}^{M} \left(\mathbf{b}_j \cdot \frac{(\mathbf{b}_j + \mathbf{n}_j) \cdot \hat{\mathbf{b}}_1}{(\mathbf{b}_1 + \mathbf{n}_1) \cdot \hat{\mathbf{b}}_1} \hat{\mathbf{b}}_1 \right) \right). \quad (25)$$

Substituting $\mathbf{b}_j = s_{j-1}\mathbf{b}_1$ into (25), we obtain

$$\arg\max_{\hat{\mathbf{b}}_j} \left(\sum_{j=1}^{M} \left(\mathbf{b}_j \cdot \hat{\mathbf{b}}_j\right) \right) = \arg\max_{\hat{\mathbf{b}}_1} \left(\sum_{j=1}^{M} \left(s_{j-1}\mathbf{b}_1 \cdot \frac{(s_{j-1}\mathbf{b}_1 + \mathbf{n}_j)}{(\mathbf{b}_1 + \mathbf{n}_1)} \hat{\mathbf{b}}_1 \right) \right). \quad (26)$$

As mentioned above, s_{j-1} denotes the BPSK modulated symbol and thus has the value of $+1$ or -1. Considering that the noises $\mathbf{n}_1$ and $\mathbf{n}_j$ are, respectively, weakly correlated with $\hat{\mathbf{b}}_1$, we could further derive

$$\arg\max_{\hat{\mathbf{b}}_j} \left(\sum_{j=1}^{M} \left(\mathbf{b}_j \cdot \hat{\mathbf{b}}_j\right) \right) \Leftrightarrow \arg\max_{\hat{\mathbf{b}}_1} \left(\mathbf{b}_1 \cdot \hat{\mathbf{b}}_1\right). \quad (27)$$

Moreover, since $||\hat{\mathbf{b}}_1|| = ||\mathbf{b}_1|| = 1$, the maximization problem evolves into the minimization of the difference between $\hat{\mathbf{b}}_1$ and $\mathbf{b}_1$, which is represented by

$$\arg\max_{\hat{\mathbf{b}}_1} \left(\mathbf{b}_1 \cdot \hat{\mathbf{b}}_1\right) \Leftrightarrow \arg\min_{\hat{\mathbf{b}}_1} \left(\|\mathbf{b}_1\|^2 + \left\|\hat{\mathbf{b}}_1\right\|^2 - 2\mathbf{b}_1 \cdot \hat{\mathbf{b}}_1 \right) \Leftrightarrow \arg\min_{\hat{\mathbf{b}}_1} \left\| \mathbf{b}_1 - \hat{\mathbf{b}}_1 \right\|^2. \quad (28)$$

Therefore, by using (25), (27), and (28), (22) can be further derived as

$$\arg\max_{\hat{\mathbf{b}}_j} \left(\sum_{j=1}^{M} \left(\mathbf{b}_j \cdot \hat{\mathbf{b}}_j\right) \right) \Leftrightarrow \arg\min_{\hat{\mathbf{b}}_1} \left\| \mathbf{b}_1 - \hat{\mathbf{b}}_1 \right\|^2. \quad (29)$$

Thus, the problem of finding $\hat{\mathbf{B}}$ for $\arg\min_{\mathrm{rank}(\hat{\mathbf{B}})=1} \|\mathbf{R} - \hat{\mathbf{B}}\|_F$ is further converted to solving the problem $\arg\min_{\hat{\mathbf{b}}_1} ||\mathbf{b}_1 - \hat{\mathbf{b}}_1||^2$. Namely, we have

$$\arg\min_{\mathrm{rank}(\hat{\mathbf{B}})=1} \left\| \mathbf{R} - \hat{\mathbf{B}} \right\|_F \Leftrightarrow \arg\min_{\hat{\mathbf{b}}_1} \left\| \mathbf{b}_1 - \hat{\mathbf{b}}_1 \right\|^2. \quad (30)$$

So far, we have proved that by solving LRAM detection problem, namely $\arg\min_{\mathrm{rank}(\hat{\mathbf{B}})=1} \|\mathbf{R} - \hat{\mathbf{B}}\|_F$, the maximum-likelihood detection of the reference chaotic signal can be achieved, namely $\arg\min_{\hat{\mathbf{b}}_1} \|\mathbf{b}_1 - \hat{\mathbf{b}}_1\|^2$. Furthermore, in the Appendix, we provide the proof that with the aid of the maximum-likelihood detection, the minimum BER could be achieved. Thanks to the proposed maximum-likelihood detection of the reference chaotic signal, the reliability performances of MC-DCSK systems can be enhanced. Next, we will present two LRAM methods for information detections.

B. LRAM Methods for the Matrix Approximation

With considerations of the complexity, we select the SVD-based LRAM method and GLRAM method to implement the information detection. The SVD method aims to minimize the approximation error based on the principal component analysis [30] in statistics according to the matrix approximation theorem [31], whereas the GLRAM method treats data as the

native 2-D matrix patterns and employs two-sided transformations rather than the single-sided one [29].

In general, GLRAM has been verified experimentally to have better compression performance and less computation time than SVD. However, GLRAM is sensitive to large sparse noise or outliers. Accordingly, when applied in MC-DCSK receivers, the GLRAM module requires smaller buffer size and lower computational complexity. In addition, since in wireless communication systems, the noise is usually additive and follows Gaussian distribution, the GLARM-based receiver would have similar detection performances to those of the SVD-based receiver. In Sections IV-B and V, we would demonstrate the complexity analysis and BER performances of both GLRAM and SVD aided receivers.

More details about how to utilize the SVD and GLRAM methods to attain the matrix $\hat{\mathbf{B}}$ from the received noisy signal matrix $\mathbf{R}$ for MC-DCSK receivers are presented below.

1) SVD-Based LRAM Method: As presented in Section III-A, we need to obtain the estimate $\hat{\mathbf{B}}$ based on the received signal expressed as $\mathbf{R} = \mathbf{B} + \mathbf{N}$, which is the solution of $\arg\min_{\mathrm{rank}(\hat{\mathbf{B}})=1} \|\mathbf{R} - \hat{\mathbf{B}}\|_F$. Here, we will present the SVD method [31] to implement the LRAM-aided information detection.

In the SVD method, we first perform the SVD operation on the received signal matrix $\mathbf{R}$ as

$$\mathbf{R} = \mathbf{U}\mathbf{D}\mathbf{V}^T = \sum_{j=1}^{M\wedge\beta} \sigma_j \mathbf{u}_j \mathbf{v}_j^T \tag{31}$$

where $\mathbf{U}$ and $\mathbf{V}$ are orthogonal, $\mathbf{u}_j$ and $\mathbf{v}_j$ represent the jth column of $\mathbf{U}$ and $\mathbf{V}$, respectively, $M \wedge \beta$ denotes the minimum value of M and β, $\mathbf{D} = \mathrm{diag}(\sigma_1, \ldots, \sigma_r, 0, \ldots, 0)$, $\sigma_1 \geq \cdots \geq \sigma_r > 0$ and $r = \mathrm{rank}(\mathbf{R})$.

Then, the solution of $\arg\min_{\mathrm{rank}(\hat{\mathbf{B}})=k} \|\mathbf{R} - \hat{\mathbf{B}}\|_F$ can be obtained as

$$\hat{\mathbf{B}} = \mathbf{U}_k \,\mathrm{diag}(\sigma_1, \ldots, \sigma_k)\mathbf{V}_k^T \tag{32}$$

where $\mathbf{U}_k$ and $\mathbf{V}_k$ are the matrices constituted by the first k column vectors of $\mathbf{U}$ and $\mathbf{V}$, respectively, and $1 \leq k \leq r$.

For MC-DCSK receivers, as mentioned above, according to the special characteristics that the transmitted signal matrix has the rank of 1, in the SVD-based LRAM detection, we set k as one, namely $k = 1$. Then, we derive the low-rank matrix $\hat{\mathbf{B}}$ from the received matrix $\mathbf{R}$ by using (32) as

$$\hat{\mathbf{B}} = \sigma_1 \mathbf{u}_1 \mathbf{v}_1^T \tag{33}$$

where $\mathbf{u}_1 \in \mathbb{R}^{\beta\times 1}$, $\mathbf{v}_1 \in \mathbb{R}^{M\times 1}$, and $\hat{\mathbf{B}} \in \mathbb{R}^{\beta\times M}$. Since $\sigma_1 \geq \cdots \geq \sigma_r > 0$, σ_1 is the largest singular value, $\mathbf{u}_1$ and $\mathbf{v}_1$ are the corresponding singular vectors. Notably, the rank of matrix $\hat{\mathbf{B}}$ is 1, which is the same as matrix $\mathbf{B}$. Thus, with the aid of the SVD-based LRAM method, the estimate $\hat{\mathbf{B}}$ can be obtained.

2) GLRAM Method: As mentioned above, in the GLRAM method, each data point is represented as native 2-D matrix patterns, which leads to less computation time and higher compression ratio than SVD. However, different from native 2-D image data points, in the considered MC-DCSK receiver, the received data points of MC-DCSK are the columns of $\mathbf{R}$ and can only be represented as 1-D patterns.

Next, based on the GLRAM method presented in [29], we propose the improved GLRAM method for the information detection to be used at the MC-DCSK receiver. Explicitly, we formulate the problem of finding the estimates as the minimization problem as

$$\min_{\substack{\mathbf{L}\in\mathbb{R}^{\beta\times l_1}:\mathbf{L}^T\mathbf{L}=\mathbf{I}_{l_1}\\ \mathbf{P}\in\mathbb{R}^{1\times l_2}:\mathbf{P}^T\mathbf{P}=\mathbf{I}_{l_2}\\ \mathbf{Q}_i\in\mathbb{R}^{l_1\times l_2}:i=1,\ldots,M}} \sum_{i=1}^{M} \left\|\mathbf{R}_i - \mathbf{L}\mathbf{Q}_i\mathbf{P}^T\right\|_F^2 \tag{34}$$

where l_1 and l_2 are two prespecified parameters, and $\mathbf{L} \in \mathbb{R}^{\beta\times l_1}$ and $\mathbf{P} \in \mathbb{R}^{1\times l_2}$ are orthogonal matrices. Since $\mathrm{rank}(\hat{\mathbf{B}}) = 1$ is expected to be 1, l_1 and l_2 are set as $l_1 = l_2 = 1$. With the aid of the iterative algorithm given in [29], we can obtain the approximated $\mathbf{R}_i$ as $\mathbf{L}\mathbf{Q}_i\mathbf{P}^T$. Then, by approximating $\mathbf{R}_i$ for $i = 1, \ldots, M$ in the similar way, we can get the approximate estimates of the whole matrix $\mathbf{R}$.

Accordingly, the low-rank approximation of the matrix $\mathbf{R}$, i.e, $\hat{\mathbf{B}}$, can be represented as

$$\hat{\mathbf{B}} = \left(\mathbf{L}\mathbf{Q}_1\mathbf{P}^T \cdots \mathbf{L}\mathbf{Q}_M\mathbf{P}^T\right) \tag{35}$$

where $\mathbf{L}\mathbf{Q}_i\mathbf{P}^T \in \mathbb{R}^{\beta\times 1}$ for $i = 1, \ldots, M$ and $\hat{\mathbf{B}} \in \mathbb{R}^{\beta\times M}$. It is worth mentioning that with the matrices $\mathbf{L}$ and $\mathbf{P}$, the two-sided linear transformation is conducted on $\mathbf{Q}_i$.

To elaborate a bit further, since $l_1 = l_2 = 1$, the matrix $\mathbf{Q}_i \in \mathbb{R}^{1\times 1}$ actually contains only one element. Therefore, as given in (35), the approximated matrix $\hat{\mathbf{B}}$ is also a rank-1 matrix, which is in accordance with the property of $\hat{\mathbf{B}}$ obtained by using the SVD approach.

IV. Theoretical Performance Analysis

For the proposed LRAM-aided MC-DCSK receiver, we analyze the BER and prove that the LRAM-aided detection can achieve the maximum-likelihood detection of the reference chaotic signals. In addition, the complexity analysis is also provided.

A. BER Derivation

We first derive the BER expression for the proposed system over AWGN channels. From the LRAM processing presented in Section III-A, we could derive that the BER of information is closely related by the LRAM detection precision of the received chaotic signals.

Recall that at the transmitter, the transmitted information-bearing chaotic signal over the jth subcarrier can be expressed as

$$\mathbf{b}_j = s_{j-1}\mathbf{b}_1 \tag{36}$$

where $\mathbf{b}_1$ is the reference signal vector and $j = 2, 3, \ldots, M$ and s_{j-1} is the BPSK data symbol of a specific user, namely $s_{j-1} = \pm 1$.

Then, at the receiver, after the transmission over an AWGN channel, the received signal can be expressed as

$$\mathbf{b}_j + \mathbf{n}_j = s_{j-1}\mathbf{b}_1 + \mathbf{n}_j \tag{37}$$

where $\mathbf{n}_i$ is noise over the jth subcarrier.

As shown in Fig. 1(b), after the estimate $\hat{\mathbf{B}}$ is obtained, the chaotic demodulation is carried out to attain the estimate $\hat{s}_{j-1}$ of the transmitted data s_{j-1}. Namely, we have

$$\hat{s}_{j-1} = (\mathbf{b}_j + \mathbf{n}_j) \cdot \hat{\mathbf{b}}_1 = (s_{j-1}\mathbf{b}_1 + \mathbf{n}_j) \cdot \hat{\mathbf{b}}_1. \tag{38}$$

TABLE I
COMPUTATIONAL AND BUFFERING COMPARISONS

	MC-DCSK [10]	MC-DCSK-IR [22]	SA-MCDCSK [20]	LRAM with SVD	LRAM with GLRAM
Complexity	$O(\beta M)$	$O(\lambda\beta M)$	$O(\beta M)$	$O(\beta^2 M)$	$O(\beta^2 M)$
Buffering	$O(\beta M)$	$O((\beta+1)M)$	$O(\beta M)$	$O(2\beta M)$	$O((\beta+1)M)$

Next, with the aid of the Gaussian approximation methods, we can derive the BER expression over the AWGN channel by evaluating the numerical expectation and the variance of $\hat{s}_{j-1}$, which is expressed as

$$\mathrm{BER}_{\mathrm{AWGN}} = \frac{1}{2}\mathrm{erfc}\left(\frac{E\left[\hat{s}_{j-1}|s_{j-1}=+1\right]}{\sqrt{2\mathrm{var}\left[\hat{s}_{j-1}|s_{j-1}=+1\right]}}\right). \quad (39)$$

To elaborate a bit further, we can easily obtain the mean value by using (38) as

$$\begin{aligned} E\left[\hat{s}_{j-1}|s_{j-1}=+1\right] &= E\left[(\mathbf{b}_1+\mathbf{n}_j)\cdot\hat{\mathbf{b}}_1\right] \\ &= E\left[\mathbf{b}_1\cdot\hat{\mathbf{b}}_1+\mathbf{n}_j\cdot\hat{\mathbf{b}}_1\right] \\ &= E\left[\mathbf{b}_1\cdot\hat{\mathbf{b}}_1\right] \end{aligned} \quad (40)$$

where $\mathbf{n}_j$ is incoherent with $\hat{\mathbf{b}}_j$ and $E[\mathbf{n}_j\cdot\hat{\mathbf{b}}_j]=0$. For the variance, we need to take the correlation between signals into account, i.e., the variance should be the average of $j-1$ correlation values for $j=2,3,\ldots,M$ given by

$$\begin{aligned} &\mathrm{var}\left[\hat{s}_{j-1}|s_{j-1}=+1\right] = \mathrm{var}\left[\frac{1}{M-1}\sum\nolimits_{j=2}^{M}(\mathbf{b}_1+\mathbf{n}_j)\cdot\hat{\mathbf{b}}_1\right] \\ &= \mathrm{var}\left[\mathbf{b}_1\cdot\hat{\mathbf{b}}_1\right]+\mathrm{var}\left[\frac{1}{M-1}\sum\nolimits_{j=2}^{M}\left(\mathbf{n}_j\cdot\hat{\mathbf{b}}_1\right)\right]. \end{aligned} \quad (41)$$

Since $\mathbf{n}_j$ is incoherent with $\hat{\mathbf{b}}_j$ and $E[\mathbf{n}_j\cdot\hat{\mathbf{b}}_j]=0$, we can get that

$$\mathrm{var}\left[\frac{1}{M-1}\sum\nolimits_{j=2}^{M}\left(\mathbf{n}_j\cdot\hat{\mathbf{b}}_1\right)\right] = \frac{1}{M-1}\frac{N_0}{2} \quad (42)$$

where $N_0/2$ is the variance of Gaussian noise. Thus, the variance can be represented as

$$\mathrm{var}\left[\hat{s}_{j-1}|s_{j-1}=+1\right] = \mathrm{var}\left[\mathbf{b}_1\cdot\hat{\mathbf{b}}_1\right]+\frac{1}{M-1}\frac{N_0}{2}. \quad (43)$$

Thus, the BER over AWGN channel can be evaluated by

$$\mathrm{BER}_{\mathrm{AWGN}} = \frac{1}{2}\mathrm{erfc}\left(\frac{E\left[\mathbf{b}_1\cdot\hat{\mathbf{b}}_1\right]}{\sqrt{2\mathrm{var}\left[\mathbf{b}_1\cdot\hat{\mathbf{b}}_1\right]+\frac{1}{M-1}N_0}}\right). \quad (44)$$

Notably, comparing the BER expression with that of the conventional MC-DCSK system derived in [10], we can notice that the SNR in the proposed receiver increases thanks to the noise suppressing LRAM detection. Thus the proposed system would achieve better BER performances even in low SNR region. Besides, from (44), we could notice that the BER performance is determined by the mean and variance of $\mathbf{b}_1\cdot\hat{\mathbf{b}}_1$. For transmissions over fading channels, the derived BER expression could be generalized by calculating the integral of (44) with the given statistical distributions of channels.

B. Complexity Analysis

Subsequently, we analyze the complexity of the SVD-based LRAM and the GLRAM methods. In accordance with the statement the GLRAM has been verified experimentally to have better compression performance than SVD, the GLRAM module requires the buffer size of $O((\beta+1)M)$, whereas the SVD method requires the buffer size of $O(2\beta M)$. Thus, the computational complexity of the GLRAM-based receiver is slightly lower than that of the SVD-based receiver. However, when taking into account of the computation complexity of chaotic demodulations, the complexity difference is negligible. Explicitly, since the MC-DCSK received signal matrix has 1-D matrix patterns, the complexity of GLRAM will be close to that of SVD, which is $O(\beta^2 M)$.

Table I summarizes the computational and the buffering complexity of the proposed system with SVD and GLRAM, MC-DCSK [10], MC-DCSK-IR [22], and SA-MCDCSK [20] systems. In the table, λ represents the iteration number of the MC-DCSK-IR system and a low SNR will lead to a large λ. It can be seen that compared with the counterpart systems, especially with our previous research work of the MC-DCSK-IR system, the proposed LRAM-aided receiver has lower complexity at lower SNR when $\lambda > \beta$. In addition, as mentioned above, the SVD-based LRAM detector has the largest buffering complexity, whereas the GLRAM-aided receiver has similar buffering complexity to that of counterpart systems. Although the proposed LRAM aided receiver has relatively high complexity, high reliability performances could be achieved as demonstrated in the following section.

V. SIMULATION RESULTS AND ANALYSIS

In this section, the performances over AWGN channel, multipath fading channel and Rayleigh fast fading channel are investigated. We first provide and compare simulation results of BER performance for conventional MC-DCSK receiver, MC-DCSK receiver with SVD, and MC-DCSK receiver with GLRAM. Then, we simulate the relationship between the approximation error of LRAM and SNR. At last, we compare the BER performance of the proposed system, our previous research work [22] and SA-MCDCSK [20].

In accordance with the above presentations, M represents the number of subcarriers, and β denotes the spread factor, i.e., the length of the chaotic sequences. In the simulations, the parameters are set as $\beta = 50, 100$ and $M = 64, 128$. Besides, we assume that the transmitted signals experience a three-path Rayleigh fading channel, whereas the channel parameters of the three-path fading channel are set as $\mathbb{E}[h_1^2] = 4/7$, $\mathbb{E}[h_2^2] = 2/7$, $\mathbb{E}[h_3^2] = 1/7$ with variant time delays over multipath fading channels. In addition, for Rayleigh fast fading channels, we assume the channel coefficient $\mathbb{E}(h^2(t)) = 1$.

Additionally, it is worth pointing out that in the following simulations, since additive Gaussian noises are assumed to impose on the transmitted signals, the sensitivity to large sparse noise

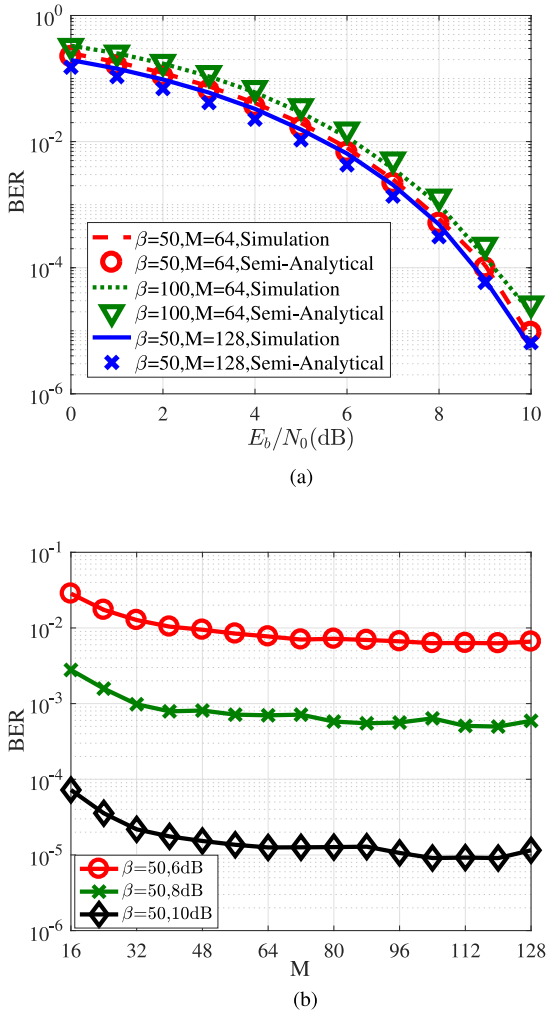

Fig. 2. BER performances of the proposed system with different M and β over AWGN channel. (a) Simulated and semianalytical BER performances. (b) BER performance versus M ($\beta = 50$).

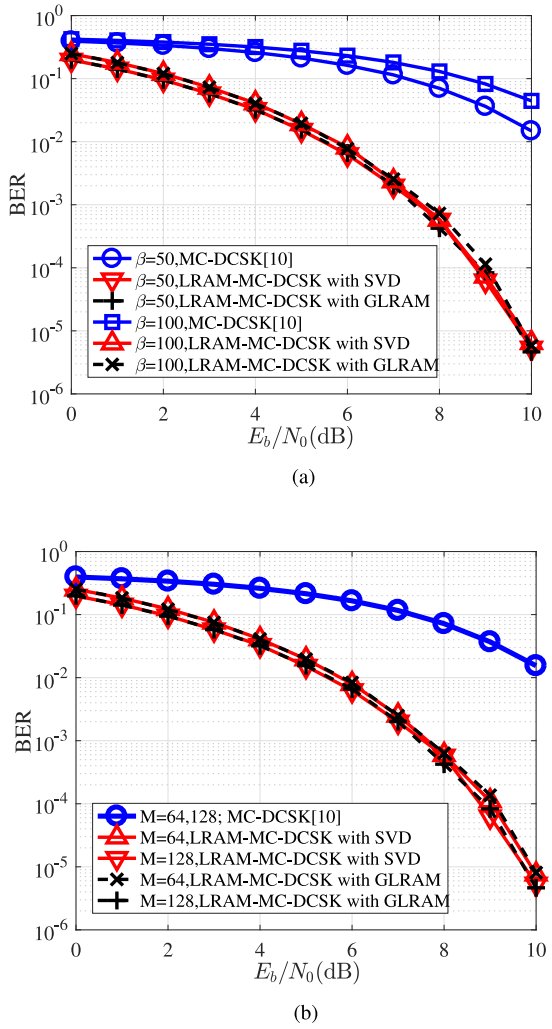

Fig. 3. BER performance comparisons over AWGN channel. (a) $M = 128$. (b) $\beta = 50$.

or outliers of the GLRAM module is not considered. Hence, the BER performances of the SVD and the GLRAM-based receivers are expected to be similar.

A. BER Performances Over AWGN Channel

First, we conduct simulations to validate the effectiveness of the derived theoretical BER expression given by (44).

Considering that the explicit expression of the statistical characteristics of $\mathbf{b}_1$ is not available, here we propose to apply the Monte Carlo method to evaluate the mean and variance value of $\mathbf{b}_1$ in (44), i.e., $E[\mathbf{b}_1 \cdot \hat{\mathbf{b}}_1]$ and $\mathrm{var}[\mathbf{b}_1 \cdot \hat{\mathbf{b}}_1]$. Since we calculate the BER by using the numerical simulated results, which are derived from the (30) to meet $\arg\min_{\hat{\mathbf{b}}_1} ||\mathbf{b}_1 - \hat{\mathbf{b}}_1||^2$ and dependent on the simulation data, the BER derived by the combination of Monte Carlo simulations and the theoretical derivations is referred to as "semianalytical" [32].

Fig. 2 compares simulated and semianalytical BER performances when using the SVD assisted LRAM method with $M = 64, 128$ and $\beta = 50, 100$. It could be observed that simulated BER results match semianalytical BER results. In addition, we could also notice from Fig. 2(a) that for the same $M = 64$ or $\beta = 50$, when β is larger or M is smaller, the BER performances degrade slightly due to the increasing interferences induced by chaotic sequences and smaller SNR. Then, from Fig. 2(b), we could notice that the BER performances are improved with larger M thanks to the noise suppressing benefit of our design. However, when M increases to 64, the BER performance gain becomes smaller with larger M due to the increasing intercarrier interferences (ICIs).

Subsequently, we compare the BER performances of the proposed LRAM aided MC-DCSK receiver, which uses the SVD and the GLRAM methods, with the benchmark MC-DCSK receiver presented in [10] over AWGN channel.

As illustrated in Fig. 3(a) and (b), in both cases that $M = 128$ with different $\beta = 50$, 100 and $\beta = 50$ with different $M = 64$, 128, the proposed SVD and GLRAM aided receivers achieve similar BER performances, which are much better than those of the counterpart MC-DCSK receiver.

Besides, we could also observe for larger value of $\beta = 100$, the BER performances are worse than $\beta = 50$ with the same $M = 128$ in Fig. 3(a), and it can also be noticed in Fig. 3(b) that

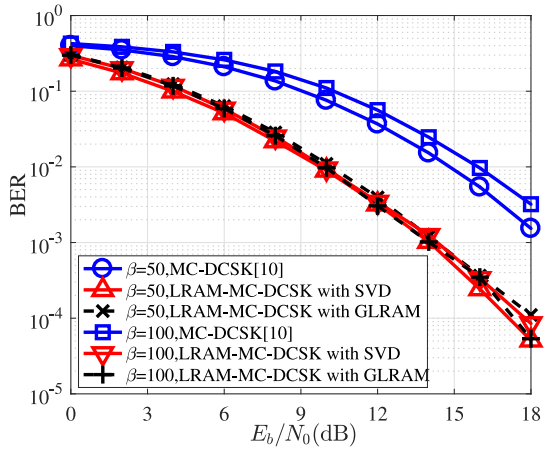

(a)

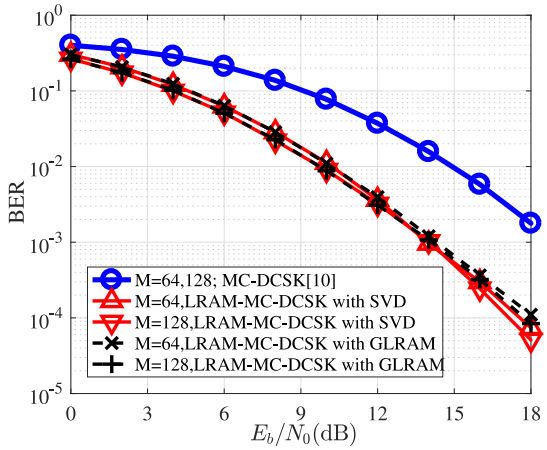

(b)

Fig. 4. Comparisons of BER performances versus E_b/N_0 over three-path fading channel with $E[h_1^2]$ =4/7, $E[h_2^2] = 2/7$, $E[h_3^2] = 1/7$ and the time delays of $\tau_1 = 0$, $\tau_2 = 3$, $\tau_3 = 6$. (a) $M = \text{128}$. (b) $\beta = \text{50}$.

the better BER performance can be attained when $M = 128$ compared with $M = 64$.

B. BER Performances Over Multipath Fading Channel

As mentioned above, we assume that a square-root-raised-cosine filter is adopted at the receiver to combat, whereas the ISI and ICI over the multipath Rayleigh fading channel [10].

Fig. 4 compares the simulated BER performances between the proposed LRAM-aided MC-DCSK receiver using the SVD and GLRAM methods, and the benchmark MC-DCSK receiver presented in [10]. As illustrated in Fig. 4(a) and (b), in both cases that $M = 128, \beta = 50$, 100 and $M = 64$, 128, $\beta = 50$, the proposed SVD and GLRAM aided MC-DCSK receivers achieve similar BER performances and outperform the benchmark MC-DCSK receiver [10]. Therefore, with the aid of the proposed LRAM-aided MC-DCSK receiver, the satisfactory BER performances can be provided for end users over multipath fading channels. Besides, we can also notice that similar to the observations over AWGN channel, the BER performances over fading channels can be improved with smaller value of β and larger value of M. Furthermore, we investigate the influence of the time delay on the

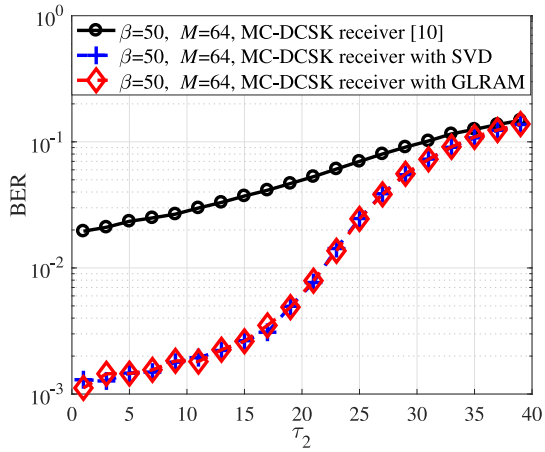

Fig. 5. Simulated BER performance versus the time delay τ_2 over three-path fading channel with $E[h_1^2] = 4/7$, $E[h_2^2] = 2/7$, $E[h_3^2] = 1/7$ and the time delays of $\tau_1 = 0$, $\tau_2 \in [1, 40]$, $\tau_3 = 6$.

BER performance. Fig. 5 provides the simulation results of BER versus the time delay over the multipath channel. The system parameters are set as $E_b/N_0 = 15$ dB, $\beta = 50$ and $M = 64$ over the three-path channels, whereas the time delays of $\tau_1 = 0$, $\tau_2 \in [1, 40]$ and $\tau_3 = \tau_2 + 1$.

As shown in Fig. 5, as the time delay increases, the performances of both the MC-DCSK receiver and the two proposed LRAM-aided MC-DCSK receivers will degrade. It is worth pointing out that for smaller τ_2, the proposed LRAM-aided MC-DCSK receiver attains better performances than the benchmark MC-DCSK receiver. However, when τ_2 increases, due to the larger delay, the performance differences between them become smaller.

C. BER Performances Over Fast Fading Channels

Fig. 6 compares the simulated BER performances between the proposed LRAM-aided MC-DCSK receiver using the SVD and GLRAM methods, and the benchmark MC-DCSK receiver presented in [10]. As demonstrated in Fig. 6, in both cases that $M = 128$ with $\beta = 50$, 100 and $\beta = 50$ with $M = 64$, 128, the proposed SVD and GLRAM associated MC-DCSK receivers achieve similar BER performances, which are better than the benchmark MC-DCSK receiver [10].

D. Analysis of Average LRAM Approximation Error

Next we investigate the estimation error of $\hat{\mathbf{b}}_1$. Note that the LRAM approximation error would determine the recovered bit energy, but would not determine the BER, which is determined by the SNR. We evaluate the LRAM approximation error by

$$e_a = \frac{1}{M}\left\|\mathbf{B} - \hat{\mathbf{B}}\right\|_F \tag{45}$$

where both $\mathbf{B}$ and $\hat{\mathbf{B}}$ are rank-1 matrices.

Fig. 7 analyzes the average LRAM precision over AWGN channel, the multipath fading channel, and fast fading channel. The channel parameters of the three-path fading channel with the time delays of $\tau_1 = 0$, $\tau_2 = 3$, $\tau_3 = 6$.

As shown from Fig. 7(a) and (b), as the SNR increases, the LRAM precision is improved. Besides, we can also notice

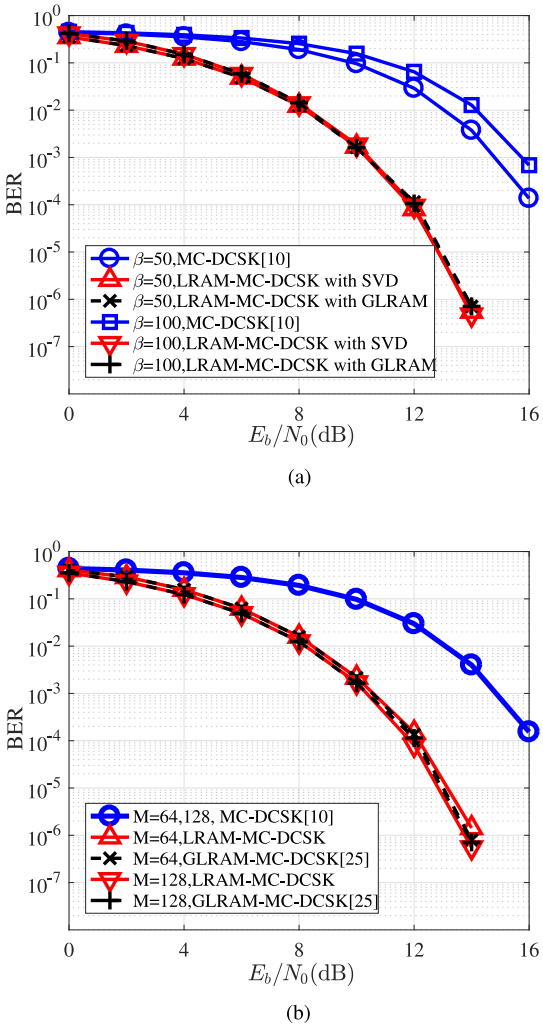

Fig. 6. Comparisons of BER performances versus E_b/N_0 over fast Rayleigh fading channels with $\mathbb{E}(h^2(t)) = 1$. (a) $M = 128$. (b) $\beta = 50$.

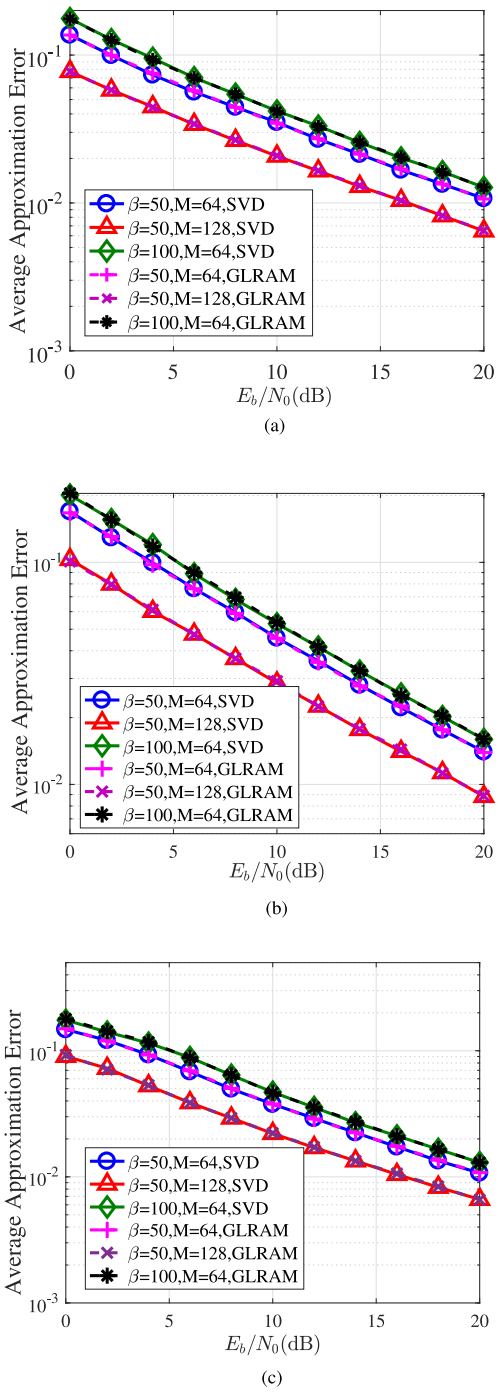

Fig. 7. Average LRAM approximation error. (a) Average LRAM precision over AWGN channel. (b) Average LRAM precision over the multipath fading channel. (c) Average LRAM precision over the fast fading channel.

that the SVD-aided LRAM method achieves similar average LRAM approximation error to that of the GLRAM method when $\beta = 50, M = 64$, $\beta = 50, M = 128$, and $\beta = 100, M = 64$. As a result, similar BER performances could be achieved by both methods, which has been demonstrated from Figs. 2–6. Additionally, it can also be seen that smaller spread factor β and larger number of subcarriers M contribute to lower average LRAM approximation error, thereby leading to improved BER performances, which is also in accordance with the observations from Figs. 2–6.

E. BER Performance Comparisons With Counterpart Systems

Next, we compare the BER performances of the proposed system, our previous work MC-DCSK-IR [22] and SA-MCDCSK [20] over AWGN channel, the multipath fading channel and Rayleigh fast fading channels when $\beta = 50, M = 64$ in Fig. 8. It could be observed from Fig. 8(a)–(c) that the proposed systems using the SVD-aided LRAM and GLRAM systems attain similar performances, which are better than those of SA-MCDCSK and MC-DCSK-IR systems. The reason is that as stated above, the LRAM methods can suppress the noises contained in both reference signals and data-bearing signals, but the MC-DCSK-IR receiver aims to improve the reliability of the reference chaotic signals via the iterations. Therefore, with aid of the SVD and GLRAM methods, the noise power reduces and thus SNR increases, thereby leading to better BER performances.

To be more explicit, from Fig. 8(a), we could observe that in order to achieve the BER of 10^{-4}, the required values of E_b/N_0 of the proposed scheme, the MC-DCSK-IR, and the SA-MCDCSK systems are, respectively, about 9, 9.2, and 11.6

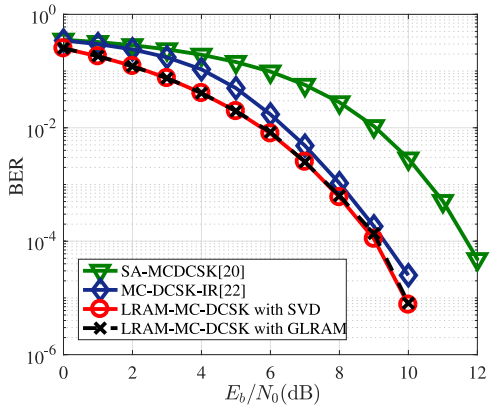

(a)

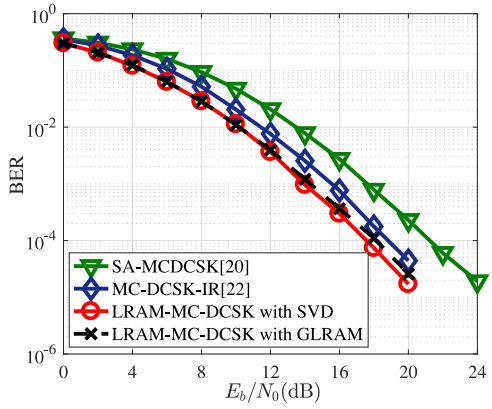

(b)

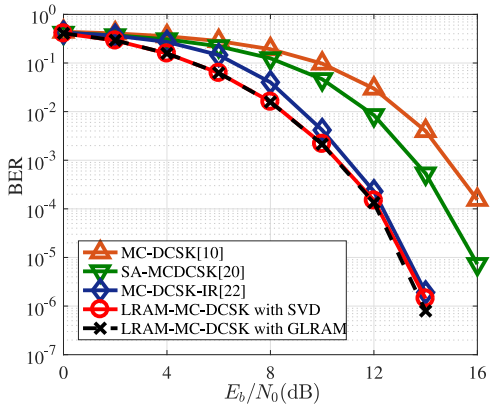

(c)

Fig. 8. BER performance comparisons of the proposed system, MC-DCSK-IR, and SA-MCDCSK over (a) AWGN channel, (b) multipath fading channel, and (c) fast fading channel. $\beta = 50$, $M = 64$.

dB. Then, from Fig. 8(b), wherein the three-path Rayleigh fading channel with time delay of $\tau_1 = 0$, $\tau_2 = 3$, $\tau_3 = 6$ is assumed, we can see that to attain the BER of 10^{-4}, the required values of E_b/N_0 of the proposed scheme, the MC-DCSK-IR, and the SA-MCDCSK systems are, respectively, about 18, 19, and 21.8 dB. At last, Fig. 8(c) shows that when E_b/N_0 of the proposed scheme, the MC-DCSK-IR, the SA-MCDCSK, and the MC-DCSK systems, respectively, achieves the value of about 12, 12, 14.6, and 16 dB, then the BER of 10^{-4} can be obtained.

VI. Conclusion

In this article, we propose a reliable LRAM-based MC-DCSK receiver design to improve the SNR of received signals. In our design, we utilize the distinctive characteristic of the MC-DCSK system that multiple chaotic modulated signals share the same reference chaotic signal. Thus, the transmitted signal matrix has low rank, and we propose to apply the LRAM methods to increase the SNR of signals and improve BER performances. Furthermore, we use the SVD and GLRAM methods to derive the approximated low-rank matrix from retrieving the estimates of the transmitted signal matrix. We prove that the problem of finding the optimal low-rank matrix can be converted to finding the optimal reference chaotic signal and that the proposed LRAM-aided receiver can achieve the maximum-likelihood detection to minimize the BER. Then the chaotic demodulation is performed to attain the information bit estimates. Simulation results demonstrate that the BER performances of the proposed LRAM aided MC-DCSK receiver are better than those of the benchmark MC-DCSK receiver and the counterpart SA-MCDCSK receiver over AWGN channel and fading channels. Furthermore, the proposed LRAM MC-DCSK receivers do not require to modify the MC-DCSK transmitter structure, and thus can be easily integrated with existing MC-DCSK systems with satisfactory practicability. Further research may include the potential applications of the proposed LRAM design in spectrum spreading systems to exploit the correlations among signals to provide improved reliability performances for users.

Appendix
Proof of Minimum BER via Maximum-Likelihood Detections

In this Appendix, we will prove that with the aid of the LRAM detection, the maximum-likelihood detection could be achieved for the reference chaotic signal.

Recall Theorem 2, the LRAM detection module will obtain $\hat{\mathbf{b}}_1$ from $\arg\max_{\hat{\mathbf{b}}_1}(\mathbf{b}_1 \cdot \hat{\mathbf{b}}_1)$.

Assuming other detection methods such as the envelop detection are used, the resultant vector is represented by $\tilde{\mathbf{b}}_1$, and $||\tilde{\mathbf{b}}_1|| = ||\hat{\mathbf{b}}_1|| = ||\mathbf{b}_1|| = 1$, then since $\hat{\mathbf{b}}_1$ is the vector to achieve the maximum value of $\mathbf{b}_1 \cdot \hat{\mathbf{b}}_1$; hence, we have

$$\mathbf{b}_1 \cdot \hat{\mathbf{b}}_1 \geq \mathbf{b}_1 \cdot \tilde{\mathbf{b}}_1. \tag{46}$$

Thereby, we can get that

$$E\left[\mathbf{b}_1 \cdot \hat{\mathbf{b}}_1\right] \geq E\left[\mathbf{b}_1 \cdot \tilde{\mathbf{b}}_1\right]. \tag{47}$$

Furthermore, since $||\tilde{\mathbf{b}}_1|| = ||\hat{\mathbf{b}}_1|| = ||\mathbf{b}_1|| = 1$, while $\hat{\mathbf{b}}_1$ will achieve the maximal correlation value with $\mathbf{b}_1$, thus we have

$$\mathrm{var}\left[\mathbf{b}_1 \cdot \hat{\mathbf{b}}_1\right] \leq \mathrm{var}\left[\mathbf{b}_1 \cdot \tilde{\mathbf{b}}_1\right]. \tag{48}$$

Therefore, according to the BER expression in (39), the application of LRAM can achieve the maximum $E[\mathbf{b}_1 \cdot \hat{\mathbf{b}}_1]$ and minimum $\mathrm{var}[\mathbf{b}_1 \cdot \hat{\mathbf{b}}_1]$, which contributes to the minimum value of $\mathrm{BER}_{\mathrm{AWGN}}$. Thus, we can draw the conclusion that

$$\arg\min_{\mathrm{rank}(\hat{\mathbf{B}})=1} \left\|\mathbf{R} - \hat{\mathbf{B}}\right\|_F \Rightarrow \arg\min_{\hat{\mathbf{b}}_1} \mathrm{BER}_{\mathrm{AWGN}}. \tag{49}$$

It is worth pointing out that (49) means that the minimum BER over AWGN channel can be attained with the $\hat{\mathbf{b}}_1$ evaluated with the proposed LRAM-aided detection scheme. Thus, the maximum-likelihood detection for received signals could be achieved.

REFERENCES

[1] J. Kim, B. Van Nguyen, H. Jung, and K. Kim, "TH-NRDCSK: A noncoherent time hopping chaotic system for anti-jamming communications," *IEEE Access*, vol. 7, pp. 144710–144719, 2019.

[2] F. C. M. Lau and C. K. Tse, *Chaos-Based Digital Communication Systems: Operating Principles, Analysis Methods and Performance Evaluation*. Berlin, Germany: Springer, 2003.

[3] R. Vali, S. Berber, and S. K. Nguang, "Accurate derivation of chaos-based acquisition performance in a fading channel," *IEEE Trans. Wireless Commun.*, vol. 11, no. 2, pp. 722–731, Feb. 2012.

[4] H. Dedieu, M. P. Kennedy, and M. Hasler, "Chaos shift keying: Modulation and demodulation of a chaotic carrier using self-synchronizing Chua's circuits," *IEEE Trans. Circuits Syst. II, Analog Digit. Signal Process.*, vol. 40, no. 10, pp. 634–642, Oct. 1993.

[5] F. C. Lau and C. K. Tse, "On optimal detection of noncoherent chaos-shift-keying signals in a noisy environment," *Int. J. Bifurcation Chaos*, vol. 13, no. 6, pp. 1587–1597, 2003.

[6] G. Kolumbán, M. P. Kennedy, and L. O. Chua, "The role of synchronization in digital communications using chaos. II. Chaotic modulation and chaotic synchronization," *IEEE Trans. Circuits Syst. I, Fundam. Theory Appl.*, vol. 45, no. 11, pp. 1129–1140, Nov. 1998.

[7] M. Sushchik, L. S. Tsimring, and A. R. Volkovskii, "Performance analysis of correlation-based communication schemes utilizing chaos," *IEEE Trans. Circuits Syst. I, Fundam. Theory Appl.*, vol. 47, no. 12, pp. 1684–1691, Dec. 2000.

[8] T. Huang, L. Wang, W. Xu, and G. Chen, "A multi-carrier M-Ary differential chaos shift keying system with low PAPR," *IEEE Access*, vol. 5, pp. 18793–18803, 2017.

[9] G. Kaddoum, F. Gagnon, and F.-D. Richardson, "Design of a secure multi-carrier DCSK system," in *Proc. 9th Int. Symp. Wireless Commun. Syst*, 2012, pp. 964–968.

[10] G. Kaddoum, F.-D. Richardson, and F. Gagnon, "Design and analysis of a multi-carrier differential chaos shift keying communication system," *IEEE Trans. Commun.*, vol. 61, no. 8, pp. 3281–3291, Aug. 2013.

[11] S. Li, Y. Zhao, and Z. Wu, "Design and analysis of an OFDM-based differential chaos shift keying communication system," *J. Commun.*, vol. 10, no. 3, pp. 199–205, 2015.

[12] G. Cheng, L. Wang, W. Xu, and G. Chen, "Carrier index differential chaos shift keying modulation," *IEEE Trans. Circuits Syst. II, Express Briefs*, vol. 64, no. 8, pp. 907–911, Aug. 2017.

[13] M. Herceg, G. Kaddoum, D. Vranješ, and E. Soujeri, "Permutation index DCSK modulation technique for secure multiuser high-data-rate communication systems," *IEEE Trans. Veh. Technol.*, vol. 67, no. 4, pp. 2997–3011, Apr. 2018.

[14] M. Herceg, D. Vranješ, G. Kaddoum, and E. Soujeri, "Commutation code index DCSK modulation technique for high-data-rate communication systems," *IEEE Trans. Circuits Syst. II, Express Briefs*, vol. 65, no. 12, pp. 1954–1958, Dec. 2018.

[15] G. Cai, Y. Fang, J. Wen, S. Mumtaz, Y. Song, and V. Frascolla, "Multi-carrier m-ary DCSK system with code index modulation: An efficient solution for chaotic communications," *IEEE J. Sel. Top. Signal Process.*, vol. 13, no. 6, pp. 1375–1386, Oct. 2019.

[16] G. Cai, Y. Fang, P. Chen, G. Han, G. Cai, and Y. Song, "Design of an MISO-SWIPT-aided code-index modulated multi-carrier M-DCSK system for e-health IoT," *IEEE J. Sel. Areas Commun.*, vol. 39, no. 2, pp. 311–324, Feb. 2021.

[17] H. Ma, G. Cai, Y. Fang, P. Chen, and G. Chen, "Design of a superposition coding PPM-DCSK system for downlink multi-user transmission," *IEEE Trans. Veh. Technol.*, vol. 69, no. 2, pp. 1666–1678, Feb. 2020.

[18] L. Zhang, Z. Chen, W. Rao, and Z. Wu, "Efficient and secure non-coherent OFDM-based overlapped chaotic chip position shift keying system: Design and performance analysis," *IEEE Trans. Circuits Syst. I, Reg. Papers*, vol. 67, no. 1, pp. 309–321, Jan. 2020.

[19] Z. Liu, L. Zhang, Z. Wu, and J. Bian, "A secure and robust frequency and time diversity aided OFDM-DCSK modulation system not requiring channel state information," *IEEE Trans. Commun.*, vol. 68, no. 3, pp. 1684–1697, Mar. 2020.

[20] H. Yang, G.-P. Jiang, W. K. Tang, G. Chen, and Y.-C. Lai, "Multi-carrier differential chaos shift keying system with subcarriers allocation for noise reduction," *IEEE Trans. Circuits Syst. II, Express Briefs*, vol. 65, no. 11, pp. 1733–1737, Nov. 2018.

[21] W. Rao, L. Zhang, Z. Zhang, and Z. Wu, "Noise-suppressing chaos generator to improve BER for DCSK systems noise-suppressing chaos generator to improve BER for DCSK systems," in *Proc. Int. Conf. Commun.*, May 2017, pp. 1–6.

[22] B. Chen, L. Zhang, and Z. Wu, "General iterative receiver design for enhanced reliability in multi-carrier differential chaos shift keying systems," *IEEE Trans. Commun.*, vol. 67, no. 11, pp. 7824–7839, Nov. 2019.

[23] O. Alter, P. O. Brown, and D. Botstein, "Singular value decomposition for genome-wide expression data processing and modeling," *Proc. Nat. Acad. Sci. USA*, vol. 97, no. 18, pp. 10101–10106, 2000.

[24] K. Konstantinides, B. Natarajan, and G. S. Yovanof, "Noise estimation and filtering using block-based singular value decomposition," *IEEE Trans. Image Process.*, vol. 6, no. 3, pp. 479–483, Mar. 1997.

[25] X. Zhou, C. Yang, H. Zhao, and W. Yu, "Low-rank modeling and its applications in image analysis," *ACM Comput. Surv.*, vol. 47, no. 2, 2015, Art. no. 36.

[26] G. Liu, Z. Lin, and Y. Yu, "Robust subspace segmentation by low-rank representation," in *Proc. 27th Int. Conf. Mach. Learn.*, 2010, pp. 663–670.

[27] T. Kohda, A. Tsuneda, and T. Sakae, "Chaotic binary sequences by Chebyshev maps and their correlation properties," in *Proc. IEEE 2nd Int. Symp. Spread Spectr. Techn. Appl.*, 1992, pp. 63–66.

[28] D. Tse and P. Viswanath, *Fundamentals of Wireless Communication*. New York, NY, USA: Cambridge Univ. Press, 2005.

[29] J. Ye, "Generalized low rank approximations of matrices," *Mach. Learn.*, vol. 61, no. 1–3, pp. 167–191, 2005.

[30] S. Wold, K. Esbensen, and P. Geladi, "Principal component analysis," *Chemometrics Intell. Lab. Syst.*, vol. 2, no. 1–3, pp. 37–52, 1987.

[31] C. Eckart and G. Young, "The approximation of one matrix by another of lower rank," *Psychometrika*, vol. 1, no. 3, pp. 211–218, 1936.

[32] N. M. S. Costa and A. V. T. Cartaxo, "Novel semi-analytical method for BER evaluation in simulated optical DQPSK systems," *IEEE Photon. Technol. Lett.*, vol. 21, no. 7, pp. 447–449, Apr. 2009.